Direct Determination of Interfacial Magnetic Moments with a Magnetic Phase Transition in Co Nanoclusters on Au(111)

T. Koide,[1] H. Miyauchi,[1] J. Okamoto,[2] T. Shidara,[1] A. Fujimori,[2] H. Fukutani,[3] K. Amemiya,[4] H. Takeshita,[5] S. Yuasa,[5] T. Katayama,[6] and Y. Suzuki[5]

[1]*Photon Factory, IMSS, High Energy Accelerator Research Organization, Tsukuba, Ibaraki 305-0801, Japan*
[2]*Department of Physics, University of Tokyo, Bunkyo-ku, Tokyo 113-0033, Japan*
[3]*Institute of Physics, University of Tsukuba, Tsukuba, Ibaraki 305-0006 Japan*
[4]*Research Center for Spectrochemistry, University of Tokyo, Bunkyo-ku, Tokyo 113-0033, Japan*
[5]*JRCAT, National Institute of Advanced Industrial Science and Technology, Tsukuba, Ibaraki 305-8568, Japan*
[6]*Department of Physics, Toho University, Funabashi, Chiba 274-0072, Japan*

(Received 8 December 2000; published 28 November 2001)

The spin, in-plane and out-of-plane orbital and magnetic dipole moments of almost purely interfacial Co atoms were directly determined for Au/2-monolayer Co nanoclusters/Au(111) by angle-dependent magnetic circular x-ray dichroism (MCXD) measurements. The field- and temperature-dependent MCXD evidences a ferromagnetic(FM)-to-superparamagnetic phase transition in single-domain clusters with decreasing size. The interfacial moments are remarkably enhanced as compared with bulk values, verifying theoretical predictions. The FM clusters show strong perpendicular magnetic anisotropy, providing promise of applications for nanoscale magnetic bits.

DOI: 10.1103/PhysRevLett.87.257201 PACS numbers: 75.50.Tt, 75.70.Cn, 78.20.Ls, 78.70.Dm

The evolution of magnetic states from the Hund's-rule-derived atomic spin to macroscopic, long-range, spin-ordered ferromagnetism is a long-standing fundamental, but not yet fully resolved, quantum-statistical problem in condensed-matter physics. The magnetism of low-dimensional systems, such as nanoclusters, ultrathin films, and multilayers, has recently attracted much interest [1–3], both because of their bridge character between 0-dimensional isolated atoms and 3-dimensional condensed systems, and because of their potential technological applications for new magnetic recording devices. Theoretical studies have predicted that the spin (m_{spin}) and orbital (m_{orb}) magnetic moments could be strongly enhanced in nanoclusters [4] as well as at surfaces and interfaces [5], as compared to those in bulk. Stern-Gerlach-deflection experiments [3,6] have shown that the magnetic moment ($m_{\mathrm{tot}} = m_{\mathrm{spin}} + m_{\mathrm{orb}}$) of Fe, Co, and Ni free clusters increases with decreasing size. An enhanced m_{orb} of Co and Fe has been reported in multilayers [7], ultrathin films [8], surfaces [9], and supported clusters [10] by magnetic circular x-ray dichroism (MCXD) measurements, although no enhanced m_{spin} has yet been reported. A direct and separate determination of m_{spin} and m_{orb} of purely surface or interface atoms still remains to be a challenge for experimentalists. Difficulty arises from requirements for samples comprising only surface or interface atoms and for highly sensitive detection of the anisotropic atomic moments in such extremely dilute systems with a simultaneous confirmation of the microscopic structure.

Recent studies using scanning tunneling microscopy (STM) in combination with the molecular-beam epitaxy (MBE) technique have revealed that supported nanoclusters are self-organized on reconstructed metal surfaces, such as Co on Au (111) and Cu (111) [11,12]. Superparamagnetism (SPM) was strongly indicated by previous experiments, but the SPM clusters cannot be applied to magnetic recording devices operating at room temperature. The most remarkable feature of Co clusters self-assembled on Au(111) is their constant height of 2 monolayers (ML), independent of the nominal Co coverage [11,12]. A natural question arises: What is the physical origin of the constant 2-ML height? This question remains unanswered. Nevertheless, if one *reverses* the problem by admitting the experimental fact, and only if Co clusters with suitable size are *capped* with an Au film (Fig. 1a), it is found that almost all of the Co atoms can be regarded as interfacial ones (a "magic height") with a negligible number of perimeter atoms. This provides an ideal system for approaching purely interfacial magnetism.

Here, we report on the first *direct* determination of m_{spin}, in-plane ($m_{\mathrm{orb}}^{\parallel}$) and out-of-plane ($m_{\mathrm{orb}}^{\perp}$) orbital moments, and in-plane ($m_T^{\parallel}$) and out-of-plane ($m_T^{\perp}$) magnetic dipole moments of almost *purely interfacial* Co atoms in Au/Co nanoclusters/Au(111) by exploiting the 2-ML height. We present evidence that the Co clusters retain ferromagnetic (FM) alignment at 300 K over a range of size, and that a FM-to-SPM phase transition takes place with decreasing size. These are achieved by angle-, field-, and temperature-dependent MCXD measurements with the first full use of a magic-angle arrangement ($\theta = 54.7°$ with $3\cos^2\theta - 1 = 0$) [13] on size-controlled, oxidation-free Co nanoclusters, with a simultaneous confirmation of the microscopic structure. We find that the interfacial m_{spin} is strongly enhanced and that m_{orb} and m_T are highly anisotropic and enhanced compared with those in bulk. By showing the strong perpendicular magnetic anisotropy of

Co clusters, we point out the possibility of an application of each single-domain FM cluster as a nanoscale magnetic bit operating at room temperature. We give its physical foundation and propose a method to realize it.

Figure 1 shows the sample structure and MCXD experimental arrangement. The sample preparation and structural characterization are described elsewhere [12]. A wedge-shaped Co, with a nominal coverage d^*_{Co} ranging from 0 to 2 ML, was grown on a heat-treated Au(111) seed layer with a mica substrate using MBE. The microscopic structure of Au and Co was characterized using STM. This revealed atomically flat, 100–200-nm wide Au(111) terraces with the "herringbone" pattern [12] and Co nanoclusters nucleated predominantly at herringbone elbow sites with an almost 2-ML height (Fig. 1b). The cluster's average in-plane diameter (D_{av}) is proportional to $\sqrt{d^*_{\mathrm{Co}}}$ [14], due to the constant height and fixed nucleation sites (Fig. 1c). The Co clusters were capped with a 2-nm-thick Au layer to ensure the "magic height" and to prevent the Co from oxidation (Fig. 1d). Angle-, field-, and temperature-dependent MCXD experiments were performed at the Co $L_{2,3}$ and the Au $N_{6,7}$ and $O_{2,3}$ edges by detecting x-ray absorption spectra (XAS) using the total-electron-yield method with circularly polarized synchrotron radiation on bending-magnet (BL-11A) and helical-undulator (BL-28A) beam lines at the Photon Factory (Fig. 1d). Magnetic fields B using a superconducting magnet were parallel and antiparallel to the photon helicity (h). The degree of circular polarization (P_C) was measured to be 92 ± 3% on BL-28A and evaluated to be 78 ± 3% on BL-11A. The incidence angle θ was changed by rotation about the vertical axis, and D_{av} (or d^*_{Co}) at the light-spot position was varied by vertical translation. The temperature T was varied from 300 to 30 K. The saturation effect [15] is negligible due to the 2-ML height.

Figure 2 shows the B and T dependencies of flux-normalized, polarization-dependent, normal-incidence ($\theta = 0°$) Co $L_{2,3}$-edge XAS (μ_+ and μ_-) and MCXD ($\Delta\mu = \mu_+ - \mu_-$) spectra, and L_3 MCXD-derived hysteresis curves for different D_{av} (or d^*_{Co}). Here μ_+ and μ_- stand for the absorption coefficients for h parallel and antiparallel to the $3d$ majority-spin direction. No features typical for CoO in XAS and strong MCXD signals (Fig. 2a) rule out the presence of oxidized Co atoms. The Co clusters with $D_{\mathrm{av}} \simeq 8.2$ and 7.2 nm exhibit a fairly strong remanent MCXD at 300 K (Fig. 2a) [16] and the B-dependent MCXD shows a clear hysteresis (Fig. 2b), revealing that Co clusters with 7.2 nm $\lesssim D_{\mathrm{av}} \lesssim$ 8.2 nm retain cluster-cluster FM alignment at 300 K. The MCXD-detected magnetization is fully saturated at low fields, showing a single domain of each FM cluster. In contrast, no remanent MCXD was detected at 300 K in Co clusters with $D_{\mathrm{av}} \simeq 4$, 4.7, and 6.7 nm (see Fig. 2c for the 4.7 nm sample), whereas a strong MCXD was observed at 300 K for $B = \pm 5$ T for all of three D_{av} (see Fig. 2d for the 4 nm sample). The MCXD intensity at 300 K strongly depends on $|B|$ for $D_{\mathrm{av}} \lesssim 6.7$ nm. It can be fitted approximately by a Langevin function, indicating the SPM of small clusters with $D_{\mathrm{av}} \lesssim 6.7$ nm. The zero-field cooled, T-dependent MCXD for $D_{\mathrm{av}} \simeq 4.7$ nm clusters shows a

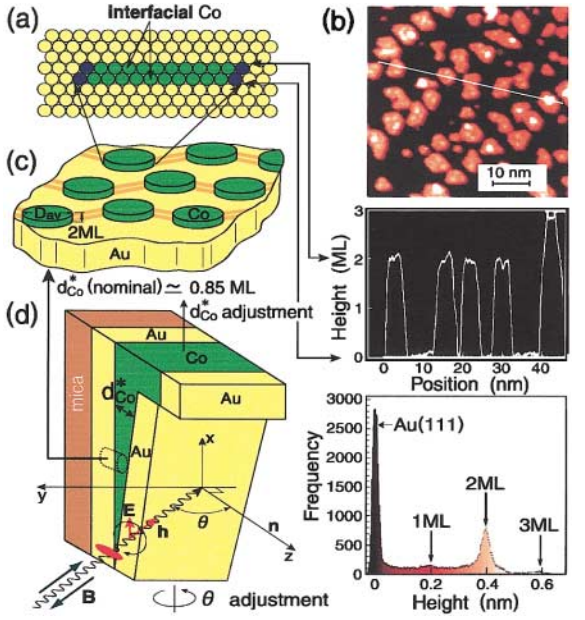

FIG. 1 (color). (a) Schematic microscopic structure for Au/2-ML Co clusters/Au(111). (b) STM picture (top), scanning height distribution along the STM white line (middle), and height distribution histograms (bottom) for $d^*_{\mathrm{Co}} \simeq 0.85$ ML ($D_{\mathrm{av}} \simeq 4.7$ nm). (c) Schematic image of independent Co clusters. (d) Nominal sample structure and arrangement for angle- and size-dependent MCXD experiments.

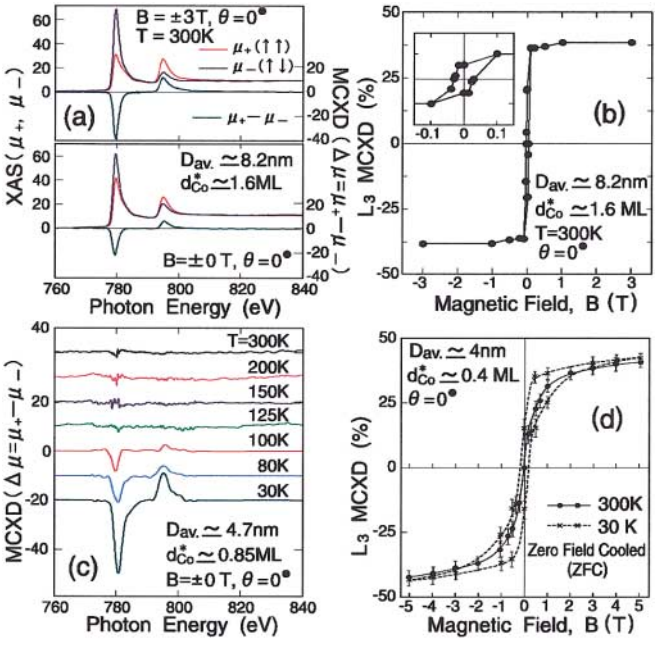

FIG. 2 (color). (a) Co $L_{2,3}$ XAS and P_C-corrected MCXD spectra of $D_{\mathrm{av}} \simeq 8.2$ nm clusters. (b) L_3-edge MCXD hysteresis curve for $D_{\mathrm{av}} \simeq 8.2$ nm at 300 K. The inset shows the expanded low-field region. (c) T-dependent Co $L_{2,3}$ remanent MCXD [16] for $D_{\mathrm{av}} \simeq 4.7$ nm. (d) L_3-MCXD hysteresis curve at 30 K and B-dependent MCXD at 300 K for $D_{\mathrm{av}} \simeq 4$ nm.

clear remanent MCXD at $T \lesssim 100$ K but no remanent MCXD for $T \gtrsim 125$ K. This shows that the magnetic moments of Co clusters are randomly oriented due to thermal fluctuations at high temperatures, and are mutually aligned ferromagnetically for $T \lesssim 100$ K, giving a blocking temperature of $T_B \simeq 100$–120 K. A similar T-dependent MCXD of $D_{\mathrm{av}} \simeq 4$ nm clusters yields $T_B \simeq 70$–80 K. The B-dependent MCXD at $T = 30$ K and 300 K for $D_{\mathrm{av}} \lesssim 6.7$ nm showed a clear hysteresis only at 30 K, whereas a saturated MCXD at $B = \pm 5$ T was nearly equal for $T = 30$ and 300 K. This reveals single domains of the Co clusters and the alignment of their moments by the external B. All of the results evidence a FM-to-SPM phase transition at $D_{\mathrm{av}}^{\mathrm{crit}} \simeq 6.7$–$7.2$ nm with decreasing D_{av}.

Figure 3 shows typical angle (θ)-resolved Co $L_{2,3}$-edge MCXD and its energy-integrated spectra. The angle-dependent MCXD sum rules [13,17] state that

$$m_{\mathrm{orb}}^{\theta} = -\frac{4[\Delta A_{L_3} + \Delta A_{L_2}]^{\theta} n_h \mu_B}{3[A_{L_3} + A_{L_2}]}, \quad (1)$$

$$m_{\mathrm{spin}} + 7m_T^{\theta} = -\frac{2[\Delta A_{L_3} - 2\Delta A_{L_2}]^{\theta} n_h \mu_B}{[A_{L_3} + A_{L_2}]}, \quad (2)$$

where A_{L_3} and A_{L_2}, and ΔA_{L_3} and ΔA_{L_2} are the L_3- and L_2-edge integrated XAS sum ($\mu_+ + \mu_-$) and MCXD intensities, respectively, n_h is the $3d$ hole number, $m_{\mathrm{orb}}^{\theta} = -\langle L_\theta \rangle \mu_B/\hbar$, $m_{\mathrm{spin}} = -2\langle S \rangle \mu_B/\hbar$, and $m_T^{\theta} = -\langle T_\theta \rangle \mu_B/\hbar$ [18] with $\langle T_\theta \rangle$ being the expectation value of the intra-atomic magnetic dipole operator $\boldsymbol{T} = \boldsymbol{S} - 3\boldsymbol{r}(\boldsymbol{r} \cdot \boldsymbol{S})/r^2$ [13,17]. Because the combined use of $m_j^{\theta} = m_j^{\parallel} \sin^2\theta + m_j^{\perp} \cos^2\theta$ (j = orb or T) and $2m_T^{\parallel} + m_T^{\perp} = 0$ [8,13] leads to $m_T^{\theta} = m_T^{\parallel}(1 - 3\cos^2\theta) = 0$ at $\theta = 54.7°$ (magic angle), Eq. (2) reduces to

$$m_{\mathrm{spin}} = -\frac{2[\Delta A_{L_3} - 2\Delta A_{L_2}]^{\theta} n_h \mu_B}{[A_{L_3} + A_{L_2}]}, \quad (3)$$

which allows a direct determination of m_{spin} [13]. The m_{spin}, $m_{\mathrm{orb}}^{\parallel}$, $m_{\mathrm{orb}}^{\perp}$, $m_T^{\parallel}$, $m_T^{\perp}$, and $m_{\mathrm{tot}} = m_{\mathrm{spin}} + (2m_{\mathrm{orb}}^{\parallel} + m_{\mathrm{orb}}^{\perp})/3$ were determined by applying sum rules (1) and (3) to the data for $\theta = 0°$ and 54.7° with the relationship between m_j^{θ}, $m_j^{\parallel}$, and $m_j^{\perp}$. The self-consistency was confirmed by the data for $\theta = 0°$ and 65°. Two independent analyses were made with no appreciable resultant difference; one used calculated n_h values for Co_2Pt_4 multilayers [19] and the other was based on determining the constant $C = (A_{L_3} + A_{L_2})/n_h$ [20].

Figure 4 shows the magnetic moments as a function of D_{av} and the number of atoms per cluster (N). m_{spin} reaches $(2.0$–$2.15)\mu_B$ for Co clusters with $D_{\mathrm{av}} \lesssim 7.2$ nm. This implies a nearly full spin polarization of the Co $3d$ electrons. These m_{spin} values are of almost *purely interfacial* Co atoms, providing the first *direct verification* of an enhanced interfacial m_{spin} predicted by theories [4,5]. The smaller values of m_{spin} and $m_{\mathrm{orb}}^{\perp}$ only for $D_{\mathrm{av}} \simeq 8.2$ nm clusters could be due to their imperfect 2-ML height [14]. The present $m_{\mathrm{tot}} \simeq 2.2$–$2.4\mu_B$ for $D_{\mathrm{av}} \lesssim 7.2$ nm agrees nicely with $m_{\mathrm{tot}} \simeq 2.4$–$2.5\mu_B$ of free Co clusters with the smallest number of atoms, obtained by Stern-Gerlach-deflection experiments [3,6]. This indicates that the present interfacial Co $3d$-Au $5d$ hybridization would be small. This is plausible, since the $5d$ band of bulk Au is located well below the Fermi level. The small

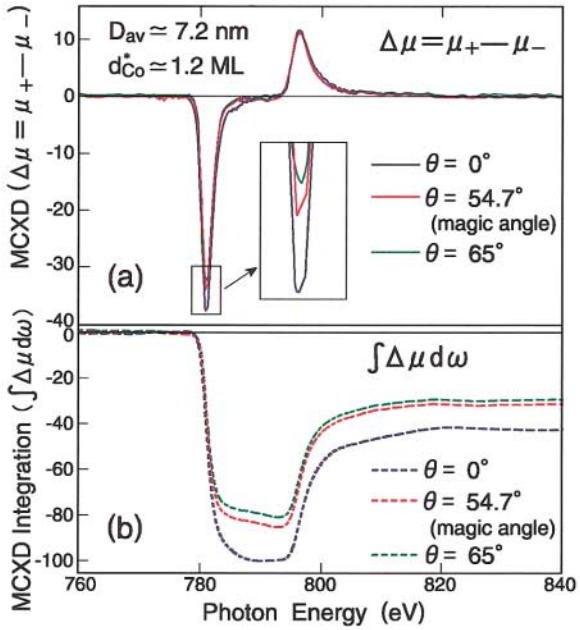

FIG. 3 (color). (a) Angle-dependent Co $L_{2,3}$ MCXD and (b) its energy-integrated spectra for FM clusters with $D_{\mathrm{av}} \simeq 7.2$ nm taken at $T = 300$ K under $B = \pm 3$ T. For SPM clusters with $D_{\mathrm{av}} \lesssim 6.7$ nm, $T = 30$ K and $B = \pm 5$ T were chosen.

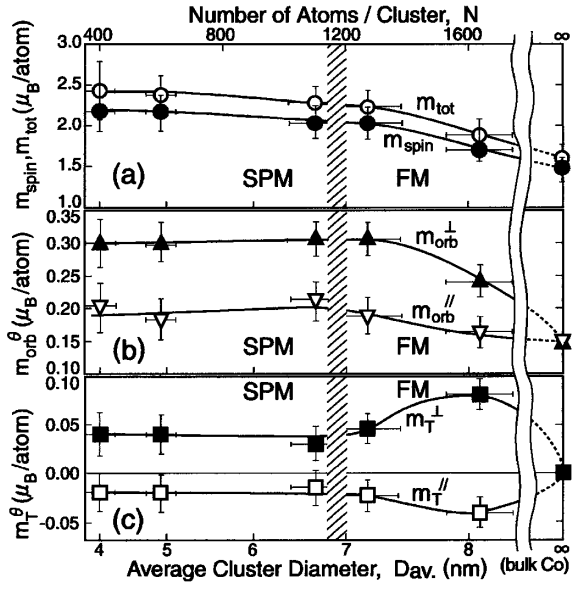

FIG. 4. D_{av} and N dependencies of (a) m_{spin} and m_{tot}, (b) $m_{\mathrm{orb}}^{\parallel}$ and $m_{\mathrm{orb}}^{\perp}$, and (c) $m_T^{\parallel}$ and $m_T^{\perp}$. The hatched area denotes the FM-to-SPM transition region. The solid curves are guides to the eye.

d-d hybridization was confirmed by the present negligibly weak Au $N_{6,7}$- and $O_{2,3}$-edge MCXD. The $m_{\rm orb}^{\perp}$ increases rapidly with decreasing $D_{\rm av}$, reaching $m_{\rm orb}^{\perp} \simeq 0.30$–$0.31\mu_B$ for $D_{\rm av} \lesssim 7.2$ nm. This value is $\sim$2 times as large as that of bulk Co, being similar to results for $m_{\rm orb}^{\perp}/m_{\rm spin}^{\rm eff}$ obtained by normal-incidence MCXD in Co clusters/Au(111) [10]. The present $m_{\rm orb}^{\perp}$ is close to $m_{{\rm orb},S}^{\perp} \simeq 0.36\mu_B$ estimated by Weller *et al.* from extrapolation to $t_{\rm Co} = 1$ ML in Au/normal Co films/Au(111), whereas our $m_{\rm orb}^{\parallel} \simeq 0.16$–$0.21\mu_B$ disagrees with their 1-ML extrapolated $m_{{\rm orb},S}^{\parallel} \approx 0$ [8]. However, this seeming discrepancy is not unexpected, since our samples were independent clusters; the $m_{\rm orb}^{\theta}$ anisotropy should disappear for $D_{\rm av}$ comparable to the cluster's height.

At the Co/Au interface, the decreased effective coordination number and the increased electron localization mainly in the perpendicular direction lead to more localized atomiclike $3d$ wave functions. This would narrow the $3d$ band width, resulting in a transfer of the electron occupation number from the minority- to majority-spin bands while nearly keeping the total hole number. This could cause an enhancement of $m_{\rm spin}$. A symmetry reduction at interfaces produces a strong uniaxial crystal field and lifts the orbital degeneracy, thus enhancing the different occupations of the in-plane and out-of-plane $3d$ orbitals. This produces an $m_{\rm orb}^{\perp}$ enhancement [7] and a nonzero anisotropic m_T^{θ} [8]. The nonvanishing m_T^{θ} shows a partial manifestation of the intrinsic quadrupole moment in the electron-density distribution $\langle Q_{\theta\theta}\rangle$ of each $3d$ orbital, since m_T^{θ} is related with $\langle Q_{\theta\theta}\rangle$ by $m_T^{\theta} \propto -\langle T_{\theta}\rangle \approx \langle Q_{\theta\theta}\rangle \cdot \langle S\rangle$ [13].

We estimate a perpendicular magnetic anisotropy energy caused by the spin-orbit (SO) interaction using $m_{\rm orb}^{\perp}$ and $m_{\rm orb}^{\parallel}$ and the majority-hole corrected Bruno's relationship $\Delta E_{\rm SO} \approx -\alpha\xi_{3d}(m_{\rm orb}^{\perp} - m_{\rm orb}^{\parallel})/(4\mu_B)$ [21,22]. By using $\alpha \approx 0.2$ [8,22] and a SO constant $\xi_{3d} \approx 70$ meV for Co, we obtain $\Delta E_{\rm SO} \approx -4.2 \times 10^{-4}$ eV/atom and $\Delta E_{\rm SO} \approx -2.5 \times 10^{-4}$ eV/atom for the FM clusters with $D_{\rm av} \simeq 7.2$ nm and $D_{\rm av} \simeq 8.2$ nm, respectively. The spin-spin dipole interaction energy, which favors the in-plane magnetic anisotropy, was calculated to be $2\pi {\rm M}_s^2 \times 0.93 \approx +0.86 \times 10^{-4}$ eV/Co atom [23]. We find that $|\Delta E_{\rm SO}| > 2\pi {\rm M}_s^2 \times 0.93$, which shows strong perpendicular magnetic anisotropy (PMA) of the FM clusters with $|\Delta E_{\rm SO}| \approx (23$–$30)k_BT$/cluster for $T = 300$ K. Thus, the present Co nanoclusters in the range of $7.2 \lesssim D_{\rm av} \lesssim 8.2$ nm have four important properties: no oxidation, single domains, FM at 300 K, and PMA. The magnetic moment of each cluster may be reversed by modern atom technologies, such as magnetic force microscopy (MFM) with an appropriate tip's radius of curvature and a suitable magnetic-field strength. Its reversed moment may be held after the MFM tip is removed, because the spin flip requires an energy larger than the reorientation energy barrier. If the cluster-cluster FM-interaction energy is smaller than the energy barrier, the single cluster's "antiparallel" spin would be maintained. Therefore, the present FM Co clusters may provide a technological possibility for utilizing each cluster as a nanoscale magnetic bit operating at 300 K.

In conclusion, we have directly determined $m_{\rm spin}$, $m_{\rm orb}^{\parallel}$, $m_{\rm orb}^{\perp}$, $m_T^{\parallel}$, $m_T^{\perp}$, and $m_{\rm tot}$ of almost purely interfacial Co atoms and presented evidence for a FM-to-SPM phase transition in Au/Co nanoclusters/Au(111). We have pointed out the possibility of the room-temperature application of Co clusters as nanoscale magnetic bits.

The authors thank Professor H. Sugawara and Professor H. Kobayakawa for financial support and encouragement. They acknowledge Professor J. Stöhr, Dr. H. A. Dürr, and Dr. K. Koike for stimulating discussion.

[1] *Ultrathin Magnetic Structures I and II,* edited by J. A. C. Bland and H. Heinrich (Springer-Verlag, Berlin, 1994).
[2] *Magnetic Properties of Fine Particles,* edited by J. L. Dormann and D. Fiorani (North-Holland, Amsterdam, 1992).
[3] I. M. L. Billas *et al.,* Science **265**, 1682 (1994); J. Shi *et al., ibid.* **271**, 937 (1996).
[4] G. M. Pastor *et al.,* Phys. Rev. Lett. **75**, 326 (1995); J. Guevara *et al., ibid.* **81**, 5306 (1998).
[5] S. Blügel *et al.,* Phys. Rev. Lett. **68**, 851 (1992); A. M. Niklasson *et al.,* Phys. Rev. B **59**, 6373 (1999).
[6] J. P. Bucher *et al.,* Phys. Rev. Lett. **66**, 3052 (1991); S. E. Aspel *et al., ibid.* **76**, 1441 (1996).
[7] Y. Wu *et al.,* Phys. Rev. Lett. **69**, 2307 (1992); N. Nakajima *et al., ibid.* **81**, 5229 (1998).
[8] D. Weller *et al.,* Phys. Rev. Lett. **75**, 3752 (1995).
[9] M. Tischer *et al.,* Phys. Rev. Lett. **75**, 1602 (1995).
[10] H. A. Dürr *et al.,* Phys. Rev. B **59**, R701 (1999); K. W. Edmonds *et al., ibid.* **60**, 472 (1999).
[11] B. Voigtländer *et al.,* Phys. Rev. B **44**, 10 354 (1991); J. de la Figuera *et al., ibid.* **47**, 13 043 (1993).
[12] H. Takeshita *et al.,* Appl. Phys. Lett. **68**, 3040 (1996); J. Magn. Magn. Mater. **165**, 38 (1997).
[13] J. Stöhr and H. König, Phys. Rev. Lett. **75**, 3748 (1995).
[14] The $d_{\rm Co}^{*} \simeq 0.85$ ML clusters have a proportional coefficient slightly different from that for other $d_{\rm Co}^{*}$ clusters. STM observations in the highest $d_{\rm Co}^{*}$ region showed predominant 2-ML but nonnegligible 3-ML height clusters.
[15] R. Nakajima *et al.,* Phys. Rev. B **59**, 6421 (1999).
[16] The remanent MCXD for $B = \pm 0$ T at temperature T was taken by changing B such that $B = 0$ T $\rightarrow +5$ T $\rightarrow +0$ T (μ_- taken) $\rightarrow -5$ T $\rightarrow -0$ T (μ_+ taken).
[17] B. T. Thole *et al.,* Phys. Rev. Lett. **68**, 1943 (1992); P. Carra *et al., ibid.* **70**, 694 (1993).
[18] We adopt here a sign convention of $m_T^{\theta} = -\langle T_{\theta}\rangle\mu_B/\hbar$ opposite to that in [8]. We have replaced $(\mu_+ + \mu_0 + \mu_-)$ by $3(\mu_+ + \mu_-)/2$ in the denominator of Eqs. (1) and (2), which could be well valid for the magic angle where linear dichroism should vanish.
[19] G. Y. Guo *et al.,* Phys. Rev. B **50**, 3861 (1994).
[20] C is proportional to the square of the $2p \rightarrow 3d$ radial transition matrix element.
[21] P. Bruno, Phys. Rev. B **39**, 865 (1989).
[22] J. Stöhr, J. Magn. Magn. Mater. **200**, 470 (1999); G. van der Laan, J. Phys. Condens. Matter **10**, 3239 (1998).
[23] The factor of 0.93 is due to the finite 2-ML height.